Original

# Enantioseparation in the Vicinity of Compensation Temperature

Masato Kazusaki* and Yasutaka Ohgami

*Analysis Laboratories, Group 1,Technology Research and Development Center Dainippon Sumitomo Pharma Co., Ltd.*

*Received for review August 23, 2007, Accepted November 19, 2007.*

**Abstract**

Extra–thermodynamic study on enantioseparation was carried out with *N*–carbobenzyloxy–D,L–leucine on amylose tris (3,5–dimethylbenzoate)coated on silica as the chiral stationary phase and a mixture of acetonitrile and phosphate buffer as the mobile phase at different column temperatures. Modification of mobile phase composition had a little impact on separation factor between enantiomers. The van't Hoff plots of retention factor and separation factor were linear over the temperature range studied. Enthalpy–entropy compensation for enantioseparation was formally established by the methods proposed by Krug *et al*. Compensation temperature for enantioseparation was calculated to be 69.4 °C, indicating nearly–constant values of the difference in Gibbs free energy change over the usable column temperature range.

*Keywords :* amylose tris (3,5–dimethylbenzoate), Chiralpak AD–RH, compensation temperature, enthalpy–entropy compensation.

## 1. Introduction

A large percentage of commercial and investigational pharmaceutical compounds are enantiomers, and many of them show significant enantioselective differences in their pharmacokinetics and pharmacodynamics. With increasing evidence of problems related to stereoselectivity in drug action, enantioselective analysis by chromatographic methods has become the focus of intensive research of separation scientists [1–4].

Great efforts have been devoted to the development of better methodology for enantioselective chromatography, and have resulted in new chiral stationary phases. Chiral stationary phases composed with polysaccharide (*e.g.*, cellulose and amylose) could separate the enantiomers by the steric fit of the molecules in the chiral cavity. Cellulose–derivative chiral stationary phases and amylose–derivative ones could separate racemic compounds in a complementary style. These columns are also acknowledged to separate wide range of racemic compounds, and commercially available all over the world [5]. However, the detailed mechanism for enantioseparation is yet to be resolved, because the intimate structure of the analyte binding site on the chiral stationary phase has not be elucidated at a molecular level.

The effect of temperature is important for understanding chromatographic behavior of analytes and characteristics of the stationary phase [6, 7]. This is especially true for enantiomeric separation. Variation of column temperature has an effect on retention and enantioselectivity of chiral analytes on a chiral stationary phase. With decreasing column temperature, enantioselectivity may either increase or decrease depending on the type of chiral discrimination mechanism based on the chiral stationary phase [8–10]. Adjustment and control of temperature are therefore useful for optimizing chiral separation [11].

By varying column temperature, thermodynamic studies were carried out to understand mechanisms of chiral recognition [12–16]. Peter *et al*. investigated temperature effects on retention of

**Correspondence :** Analysis Laboratories, Group 1, Technology Research and Development Center Dainippon Sumitomo Pharma Co., Ltd. 1–5–51 Ebie, Fukushima–ku, Osaka, 553–0001, Japan

**Tel :** +81–6–6454–8177

**Fax**：+81–6–6458–3723

**E–mail :** masato–kazusaki@ds–pharma.co.jp

enantiomers on a teicoplanin and a ristcetin chiral stationary phase [17, 18]. Oberleitner *et al*. studied the temperature influences on enantioseparation characteristics of *N*–acylated amino acids on a quinine based chiral stationary phase [19]. Weng *et al*. evaluated thermodynamic characteristics of amino acid derivatives on a tartardiamide based chiral stationary phase [20].

The present work has carried out to determine the thermodynamic parameters for enantioseparation of derived D,L–leucine as a model racemic compound, and to use this information to optimize the HPLC operating condition.

## 2. Experimental

### 2.1. Chemicals and reagents

Acetonitrile of HPLC grade, potassium dihydrogen phosphate, potassium nitrate and uracil were obtained from Wako Pure Chemical Industries Ltd. (Osaka, Japan). Water was deionized prior to usage. Potassium dihydrogen phosphate was dissolved in deionized water, and phosphoric acid was added to make 20 m*M* phosphate buffer at pH 3.0.*N*–carbobenzyloxy–D,L–leucine (*N*–CBZ–D,L–Leu) and *N*–carbobenzyloxy–L–leucine (*N*–CBZ–L–Leu) from Tokyo Kasei Kogyo Co., Ltd. (Tokyo, Japan) were of above 96.0% purity. Derived amino acids (Figure 1) were dissolved in acetonitrile at 0.1 mg/mL for chiral HPLC analysis. The L–enantiomer was employed for the identification of elution order of enantiomers. Uracil was used as a void volume marker. Acetonitrile was employed as organic modifier due to the poor durability of the chiral HPLC column for pressure.

### 2.2. Apparatus

The chromatographic system used consisted of a D–7000 System (Hitachi, Tokyo, Japan) equipped with two isocratic pumps (L–7100), variable wavelength detector (L–7420), variable volume injector (L–7200) and column oven (L–7300) equipped with column cooler. The chiral HPLC column containing amylose–derived chiral stationary phase (amylose tri–3,5–dimethylbenzoate) (4.6 mm in inside diameter and 15 cm in length with 10 μm in particle diameter) was purchased from Daicel Chemical Industries, Ltd. (Osaka, Japan). The mobile phase consisted of 20 mM phosphate buffer at pH 3.0 and acetonitrile. Acetonitrile content was set at 25 v/v %, 30 v/v %, 35 v/v %, 40 v/v % and 45 v/v %, and delivered at a flow–rate of 0.5 mL $min^{-1}$. The column temperature was adjusted at 25.0–45.0°C, and the precision of the column temperature adjustment was ± 0.1°C. The injection volume was set at 5 μL. Duplicate analyses were carried out at each column temperature. The elution of *N*–CBZ–D–Leu and *N*–CBZ–L–Leu was monitored at 220 nm. The chromatographic system was equilibrated by passing the mobile phase until a stable baseline signal was obtained.

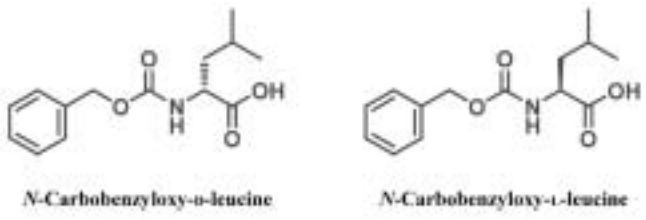


**Figure 1.** Chemical structures of *N*–carbobenzyloxy–D–leucine and *N*–carbobenzyloxy–L–leucine.

### 2.3. Thermodynamic properties of liquid chromatography

The effect of temperature on the retention is related to the change of Gibbs free energy of the equilibrium and is expected by the van't Hoff equation [21–24]. The retention and separation factors, and thermodynamic parameters for the retention and separation of two enantiomers on the amylose–derived chiral stationary phase is expressed by the following Eqs. (1)–(5), where the subscripts L and D correspond to *N*–CBZ–L–Leu (first eluted enantiomer) and *N*–CBZ–D–Leu (second eluted enantiomer), respectively :

$$\Delta\Delta G = \Delta G_D - \Delta G_L = -RT \ln \alpha = -RT \ln k_D/k_L \quad (1)$$

$$\Delta\Delta G = \Delta G_D - \Delta G_L = (\Delta H_D - T\Delta S_D) - (\Delta H_L - T\Delta S_L) = \Delta\Delta H - T\Delta\Delta S \quad (2)$$

$$\ln k_D = -\Delta H_D/RT + \Delta S_D/R + \ln \Phi \quad (3)$$

$$\ln k_L = -\Delta H_L/RT + \Delta S_L/R + \ln \Phi \quad (4)$$

$$\ln \alpha = \Delta\Delta H/RT + \Delta\Delta S/R \quad (5)$$

where $\Delta G$, $\Delta H$ and $\Delta S$ are the Gibbs free energy change, the molar enthalpy change, and molar entropy change, $\Delta\Delta G$, $\Delta\Delta H$ and $\Delta\Delta S$ are the differences in the Gibbs free energy change, the molar enthalpy change, and molar entropy change, respectively. $R$ is the gas constant, and $T$ represents the absolute temperature in Kelvin. The van't Hoff plots of ln $k$ versus $1/T$ (Eqs. (3) and (4)), ln $\alpha$ versus $1/T$ (Eq.(5)) were used to evaluate the temperature influence on retention and enantioseparation of amino acid derivatives on the amylose–derived chiral stationary phase. These plots are linear if enthalpy term and entropy term do not vary significantly within the temperature range studied.

## 3. Results and discussion

The mechanism underlying enantioseparation using derivatized polysaccharide phase is a difficult process to understand due to the complexity of nature of the polymeric stationary phase. In an effort to describe some of these processes, the separation of *N*–CBZ–D,L–Leu was studied on a tris (3,5–dimethylbenzoate) amylose phase (Chiralpak AD–RH). Enantioseparation of *N*–DBZ–D,L–Leu was carried out with this column. Representative chromatogram is shown in Figure 2. Enantioseparation was evaluated by independently varying the acetonitrile volume fraction in the mobile phase from 25 v/v % to 45 v/v % and the column temperature (25.0–45.0°C).

**Influence of acetonitrile volume fraction in the mobile phase.**

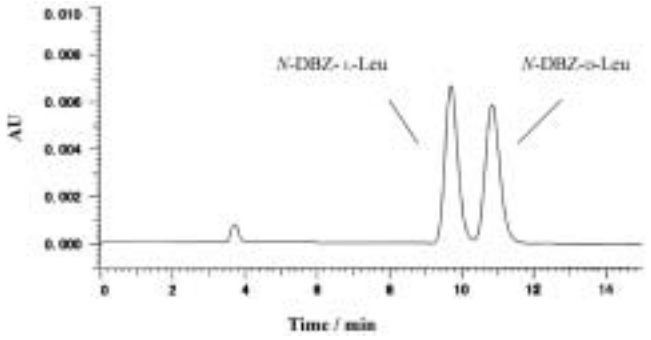


**Figure 2.** Chromatogram of *N*–DBZ–D,L–Leu on the amylose–derived chiral stationary phase. Column, Chiralpak AD –RH ; mobile phase, a mixture of phosphate buffer and acetonitrile (60/40 v/v%) ; detection, UV 220 nm ; column temperature, 25°C ; flow rate,0.5 mL min$^{-1}$.

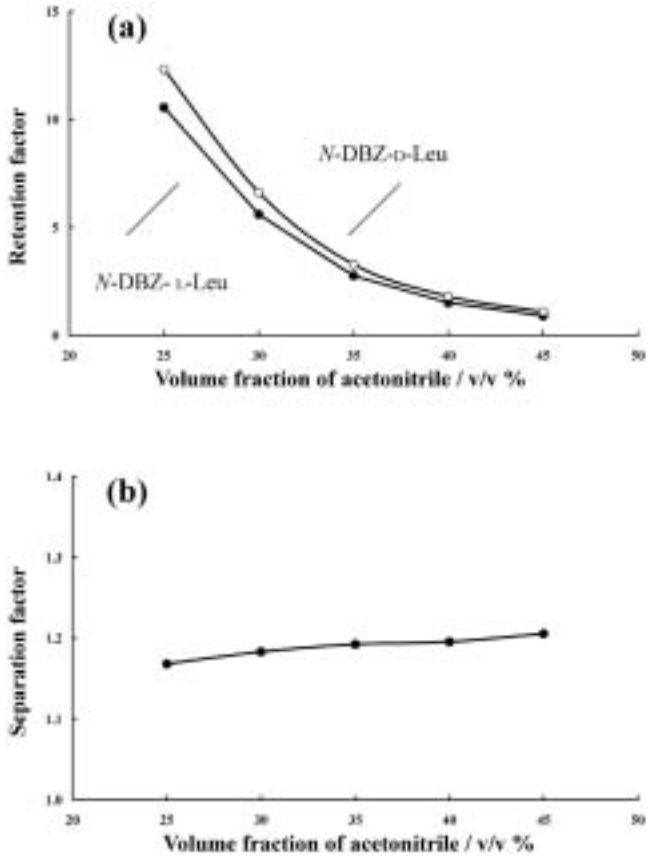


**Figure 3.** Influence of volume fraction of acetonitrile on (a) retention and (b) separation of *N*–CBZ–D–Leu and *N*–CBZ –L–Leu. Column, Chiralpak AD–RH ; mobile phase, a mixture of phosphate buffer and acetonitrile ; detection, UV 220 nm ; column temperature, 25°C ; flow rate, 0.5 mL min$^{-1}$.

To study the influence of volume fraction of organic modifier on retention factors and separation factors, acetonitrile volume fraction in the mobile phase was varied between 25 v/v % and 45 v/v % at the column temperature of 25.0°C. Plots of retention factor and separation factor versus acetonitrile content are presented in Figure 3. As shown in Figure 3(a), increment of acetonitrile content in the mobile phase exponentially reduced retention factor at a given temperature. Interestingly, separation factor was essentially unchanged over the entire range of acetonitrile content at a given temperature (Figure 3(b)).

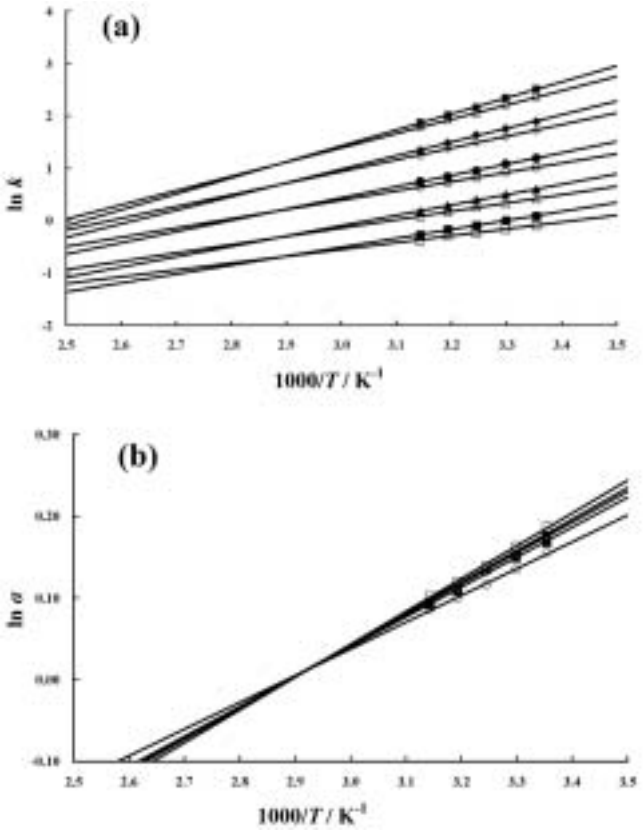


**Figure 4.** van't Hoff plots for (a) retention and (b) separation factor of *N*–CBZ–D,L–Leu. Column, Chiralpak AD–RH ; mobile phase, a mixture of phosphate buffer and acetonitrile {acetonitrile content : 25 v/v% (small square), 30 v/v % (rhomboid), 35 v/v % (circle), 40 v/v % (triangle), 45 v/v % (large square)} ; detection, UV 220 nm ; column temperature, 25–45°C ; flow rate, 0.5 mL min–1.Retention factors of *N*–CBZ–D–Leu and *N*–CBZ–L–Leu are expressed in the open symbol and closed symbol, respectively.

**Influence of temperature.** The characteristics of the retention and separation factors with the variation of column temperature can be estimated based on the plots of the natural logarithm of the retention factor of the two enantiomers or the separation factor against the reciprocal of absolute temperature (known as van't Hoff plot), respectively. These plots are depicted in Figure 4. In Figure 4(a), the five set of two lines generated from enantiomeric pairs intersect at a certain temperature (isoelution temperature), respectively, where the difference of free energy change is zero and the separation of enantiomers is not observed. It is obvious from Figure 4(a) that the mass transfer from the mobile phase to the stationary phase

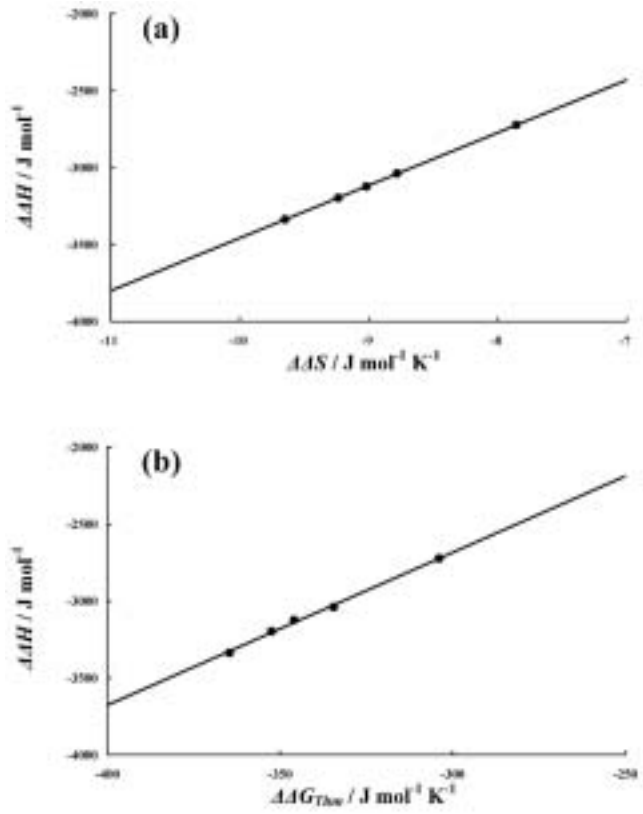


**Figure 5.** Linear correlation between (a) the differences of enthalpy change and entropy change and (b) the difference of enthalpy change and that of free energy change at compensation temperature obtained from the enantioseparation of *N*–CBZ–D,L–Leu.

is exothermic. It is also apparent that van't Hoff plots of *N*–CBZ–D–Leu and those of *N*–CBZ–L–Leu gradually assemble with increasing temperature, respectively. Temperature at which some van't Hoff plots converge is designated as compensation temperature. In many cases, the compensation temperature is typically well above the temperature region normally used for liquid chromatography [25, 26] and consequently the retention factors of most analytes increase as the column temperature decrease.

In a previous study, it was observed that the van't Hoff plots generated on the amylose–derived chiral stationary phase was non–linear with break below 20°C. This phenomenon was concluded that the stationary phase was underwent the conformational change [8]. In contrast, linear van't Hoff plots of $k$ and $\alpha$ were obtained in this study. This result indicates that the conformational change of the stationary phase was not occurred, and the mechanisms for retention and separation were not changed within the temperature range studied (25–40°C).

Figure 5(a) shows the correlation between thermodynamic parameters ($\Delta\Delta H$ and $\Delta\Delta S$) calculated from the van't Hoff plots in Figure 4(b). It also appears that the difference of enthalpy change correlates well with that of entropy change. This phenomenon is so–called "enthalpy–entropy compensation (EEC)." The slope in Figure 5(a) is designated as compensation temperature for enantioseparation.

**Enthalpy–entropy compensation.** Apparent EEC concerning enantioseparation was observed by HPLC method in this study. However, Krug *et al*. criticized this procedure harshly, and proposed four methods. These methods were applied to find out whether observed EEC was based on the substantial physico–chemical effects or results merely from a statistical compensation due to experimental errors [27–29]. Details of these four elements are described below.

(i) If EEC is actually present, the plot generated from enthalpy term and Gibbs free energy term at the harmonic mean of the experimental temperature ($\Delta\Delta G_{T\mathrm{hm}}$) will be linear. As shown in Figure 5 (b), $\Delta\Delta H$ and $\Delta\Delta G_{T\mathrm{hm}}$ correlate well with correlation coefficient of 0.997, indicating the good linearity.

(ii) Krug *et al*. proposed the following equations to test the null hypothesis that $T_c$ was equal to $T_{\mathrm{hm}}$. In this study, maximum and minimum values of $T_c$ for enantioseparation at 95% confidence level are calculated by the following equations.

$$T_c(\text{minimum}) = \sum(\Delta\Delta H - \Delta\Delta\hat{H})(\Delta\Delta S - \Delta\Delta\hat{S}) / \sum(\Delta\Delta S - \Delta\Delta\hat{S})^2 - t(3,0.05)\,V(Tc)1/2$$

$$T_c(\text{maximum}) = \sum(\Delta\Delta H - \Delta\Delta\hat{H})(\Delta\Delta S - \Delta\Delta\hat{S}) / \sum(\Delta\Delta S - \Delta\Delta\hat{S})^2 + t(3,0.05)\,V(Tc)1/2$$

where $\Delta\Delta\hat{H}$ and $\Delta\Delta\hat{S}$ are the average values of $\Delta\Delta H$ and $\Delta\Delta S$, respectively. The $t$–value, $t$ (3,0.05), is the value of the Student's $t$–test for 3 of freedom degree and a confidence level of 95%. Sample statistic, $V(Tc)$, is calculated by the following equation :

$$V(Tc) = \sum(\Delta\Delta H - \Delta\Delta G_{Tc} - Tc\Delta\Delta S)^2 / 3\sum(\Delta\Delta S - \Delta\Delta\hat{S})^2$$

Compensation temperature ($Tc$) was calculated 69.4°C (343 K), and the 95% confidence interval was 58.7–80.0°C. Compensation temperature was explicitly discriminated from the harmonic mean of the experimental temperature (34.8°C). Very low temperature for compensation was obtained for enantioseparation in the reversed–phase mode. Miyabe *et al*. reported the compensation temperature of 710–1560 K with structurally–related compounds in the reversed–phase mode [21, 22, 26].

(iii) When enthalpy–entropy compensation is observed for a group eluted with different mobile phases, all of the groups have the same degree of the difference in Gibbs free energy change at compensation temperature. When separation is influenced by EEC, the van't Hoff plot must intersect at a single point. As shown in Figure 4(b), van't Hoff plots obtained in this study pass through a certain point.

(iv) Probability for the intersection of the linear regression lines was compared with that for the non–intersection on the basis of the statistical data derived by ANOVA. The probability for non–intersection was also compared with the precision of the experimental data in the same manner. The value of the mean sum of squares for

intersection ($MS_i$) divided by that of squares for non–intersection ($MS_{ni}$) is $3.5\times10^4$ is sufficiently larger than the corresponding $F$–value of 10.1. This show the probability for intersection is high compared to that for non–intersection. On the other hand, the ratio of $MS_{ni}$ to that of squares for the residuals ($MS_\varepsilon$) is $-3.4\times10^{-4}$. The negative value of $MS_\varepsilon$ is probably unreasonable. However, it seems to arise from calculation errors, which suggests that the variation due to measurement errors is quite small. The corresponding $F$–value is 3.5. In conclusion, the variation due to the non–intersection is not greater than that due to the measurement errors.

On the basis of the results described above, we can state that the true EEC takes place for enantioseparation of *N*–CBZ–D,L–Leu on the amylose–derived chiral stationary phase, originating from substantial physico–chemical effects at the 95% level of significance. The mechanism for enantioseparation is essentially identical under the HPLC operating condition in this study.

EEC for retention is conveniently expressed by the following relationship [30] :

$$\Delta H = T_c\,\Delta S + \Delta G_{Tc} \quad (6)$$

where $\Delta G_{Tc}$ denotes the Gibbs free energy change of a physico–chemical interaction at compensation temperature ($T_c$). EEC for separation is also expressed by the following relationship :

$$\Delta\Delta H = T_c\,\Delta\Delta S + \Delta\Delta G_{Tc} \quad (7)$$

Eq. (7) can be rewritten in order to express the free energy change, $\Delta G_T$, at a fixed temperature, $T$, as

$$\Delta\Delta G_T = \Delta\Delta H\,(1 - T / T_c) + \Delta\Delta G_{Tc}\,T / T_c \quad (8)$$

Eqs. (1) and (8) give the following equation :

$$\ln \alpha_T = -\Delta\Delta H/R\,(1/T - 1/T_c) - \Delta\Delta G_{Tc}/R\,T_c \quad (9)$$

This equation implies that in the vicinity of $T_c$, the natural logarithm of separation factor is practically independent of temperature.

Let us suppose that EEC for enantioseparation takes place under the several HPLC operating conditions with different mobile phases. In this instance, enantiomers are separated by the identical mechanism. Model van't Hoff plots of the separation factors of the two enantiomers on the chiral stationary phase are shown in Figure 6. Needless to say, the slope of each line is related to the difference of the enthalpy change ($-\Delta\Delta H/R$) and the intercept is related to the difference of the entropy change ($\Delta\Delta S/R$). Figure 6 indicates un–effectiveness for improving the separation of enantiomers near compensation temperature (illustrated as open symbols). As shown in Figure 3(b), separation factor is slightly increased at 25.0°C with increase of acetonitrile content in mobile phase. This experimental temperature is close to compensation temperature (69.4°C). On the other hand, it will be probably easy to achieve the better separation in the temperature range far from compensation temperature (illustrated as closed symbols).

The enthalpic and entropic contribution for enanrtioseparation at 25°C was depicted in Figure 7. Enantioselectivity for the resolution of *N*–CBZ–D,L–Leu on the amylose–derived chiral stationary phase is enthalpically governed process. According to Eq. (8), all values of $-\Delta\Delta G$ approach zero with increase of experimental temperature up to compensation temperature. Figure 7 shows that with an increase of acetonitrile content in mobile phase, $-\Delta\Delta H$ value gradually increases. However, according to EEC, the increment of $-\Delta\Delta H$ value is almost cancelled out by the increase of the value of $-\Delta\Delta S$ times temperature, resulting in the slight increment of $-\Delta\Delta G$ value. This trend was observed at all experimental temperatures studied, and as a matter of course a small amount of increment of $-\Delta\Delta$G value steadily observed with decreasing those temperatures with the same mobile phase composition.

The result of this study with the amylase–derived chiral stationary phase indicates that separation factor of enantiomers could

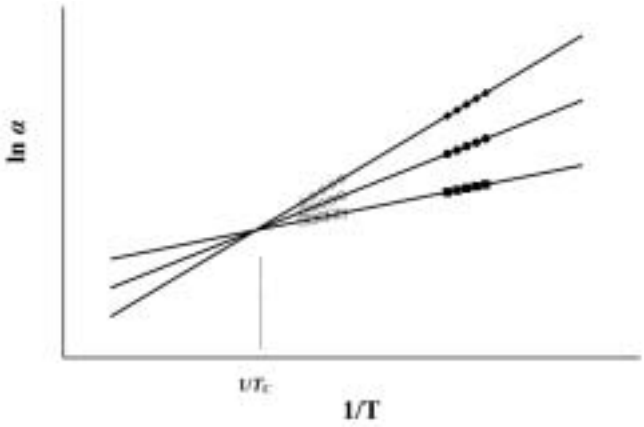


**Figure 6.** Model van't Hoff plots between ln α and 1/$T$ for enantioseparation of enantiomers on a chiral stationary phase. $T_c$ represents compensation temperature.

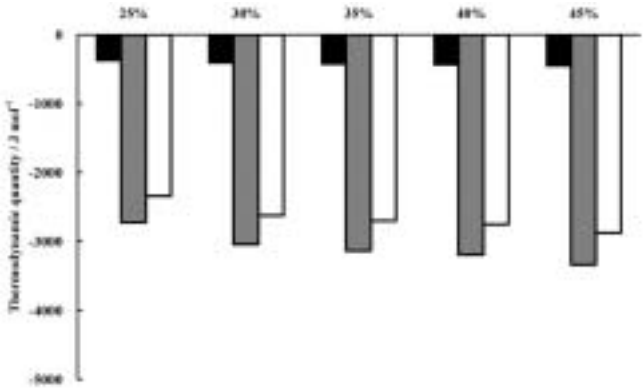

**Figure 7.** Differences in free energy change, enthalpy change and entropy change for chiral separation of derived amino acids on amylose tris (3,5–dimethylbenzoate) stationary phase at 25°C using the mobile phase of phosphate buffer – acetonitrile. The numbers on the abscissa indicate acetonitrile content in the mobile phase. Filled, unfilled and shaded parts indicate $\Delta\Delta G$, $\Delta\Delta H$, and $\Delta\Delta S$ times temperature, respectively.

not be improved drastically by lowering the experimental temperature due to the enthalpy–entropy compensation. However, measly improvement could be achieved by modifying the mobile phase composition and adjusting the experimental temperature.

**References**


[1] Caldwell, J. *J. Chromatogr. A*, **1995**, *694*, 39–48.

[2] Cadwell, J. *J. Chromatogr. A*, **1996**, *719*, 3–13.

[3] Teng, X. W. ; Wang, S. W. J. ; Davies, N. M. *J. Pharm. Biomed. Anal*. **2003**, *33*, 95–100.

[4] Brichac, J. ; Honzatko, A. ; Picklo, M. J. *J. Chromatogr. A* **2007**, *1149*, 305–311.

[5] Okamoto, Y. ; Kaida, Y. *J. Chromatogr. A* **1994**, *666*, 403–419.

[6] Persson, B.–A. ; Anderson, S. *J. Chromatogr. A* **2001**, *906*, 195–203.

[7] Dolan, J. W. *J. Chromatogr. A* **2002**, *965*, 195–205.

[8] Kazusaki, M. ; Kawabata, H. ; Matsukura, H. *J. Liq. Chromatogr. & Rel. Technol*. **2000**, *23*, 2937–2946.

[9] Kazusaki, M. ; Kawabata, H. ; Matsukura, H. J. *Liq. Chromatogr. & Rel. Technol*. **2001**, *24*, 141–151.

[10] Novak, T. J. ; Berwick, L. *J. Liq. Chromatogr. & Rel. Technol*. **1998**, *20*, 1883–1896.

[11] Chen, X.–M. ; Yamamoto, C. ; Okamoto, Y. J. *Chromatogr. A* **200**6, *1104*, 62–68.

[12] Fornstdet, T. ; Sajonz, P. ; Guiochon, G.. *J. Am. Chem. Soc*. **1997**, *119*, 1254–1264.

[13] Küsters, E. ; Spöddlin, C. *J. Chromatogr. A* **1996**, *737*, 333–337.

[14] Zang, D. *J. Chromatogr. A* **2005**, *1083*, 89–95.

[15] Buckenmainer, S. M. C. ; McCalley, D. V. ; Euerby, M. R. *J. Chromatogr. A* **2004**, *1060*, 117–126.

[16] Yang, J. ; Hage, S. J. Chromatogr. A **1996**, *725*, 273–285.

[17] Péter, A. ; Török, G., Armstrong, D. W. *J. Chromatogr. A* **1998**, *793*, 283–296.

[18] Peter, A. ; Vekes, E. ; Armstrong, D. W. *J. Chromatogr. A* **2002**, *958*, 89–107.

[19] Oberleiner, W. R. ; maier, N. M. ; Lindner, W. *J. Chromatogr. A* **2002**, *960*, 97–108.

[20] Weng, W. ; Wang, Q. H. ; yao, B. X. ; Zeng, Q. L. *J. Chromatogr. A* **2004**, *1042*, 81–87.

[21] Miyabe, K. ; Guiochon, G. *Anal. Chem*. **2002**, *74*, 5754–5765.

[22] Miyabe, K. ; Guiochon, G. *Anal. Chem*. **2002**, *74*, 5982–5992.

[23] Cheong, W. J. ; Keum, Y. I. *J. Chromatogr. A* **2001**, *910*, 195–206.

[24] Dolan, J. W. *J. Chromatogr. A* **2002**, *965*, 195–205.

[25] Kazusaki, M. ; Yamaguchi, T. *Chromatography* **2005**, *27*, 57–62.

[26] Miyabe, K. ; Guiochon, G. J. *Chromatogr. A* **2005**, *1099*, 136–148.

[27] Krug, R. R. ; Hunter, W. G. ; Grieger, R. A. *J. Phys. Chem*. **1976**, *80*, 2335–2341.

[28] Krug, R. R. ; Hunter, W. G. ; Grieger, R. A. *J. Phys. Chem*. **1976**, *80*, 2341–2351.

[29] Krug, R. R. *Ind. Eng. Chem. Fundam*. **1980**, *19*, 50–59.

[30] Vailaya, A. ; Horváth, C. *J. Phy. Chem*. **1996**, *100*, 2447–2455.